[redacted]

NRL REPORT 3730

THE FRAGMENT PENETRATION RESISTANCE OF FOUR Mg-Li-BASED ALLOY TYPES

NAVAL RESEARCH LABORATORY

WASHINGTON, D.C.

[redacted]

[redacted]

DISTRIBUTION

CNO	1
ONR	
Attn: Code 423	2
Attn: Code 463	1
BuAer	
Attn: AR-82	6
Attn: AR-41	12
BuOrd	
Attn: AD3, ReC	4
Attn: Re3, Re9	4
BuShips	
Attn: Code 300	1
Attn: Code 343	1
Attn: Code 400	1
CO & Dir., USNEL	2
CDR, USNOTS	
Attn: Reports Unit	2
Attn: Inyokern	1
Attn: Mr. John Reinhart, Penetration Dynamics	1
CO, USNPG	1
Attn: A. & P. Laboratory	1
Supt., USNGF	
Attn: 1N910	1
Attn: Mr. H. Bernstein	1
Dir., NAES	
Attn: Materials Laboratory	1
CDR, New York Naval Shipyard	
Attn: Noah Kahn, Materials Laboratory	1
CO & Dir., USNEES	
Attn: Materials Laboratory	1
OCSigO	
Attn: Ch. Eng. & Tech. Div., SIGTM-S	1
CG, SCEL	
Attn: SCEL Liaison Office	3

[redacted]

CONTENTS

ABSTRACT

The fragment-penetration resistance of four types (approximately twenty heats) of experimental magnesium-lithium-based alloy sheet is described. They were prepared under BuAer contract by the Battelle Memorial Institute for light-fragment aircraft armor studies. The fragment armor performance was measured using the NRL standard symmetrical 22-caliber yawed-dart fragment simulator. Of the alloys studied, one containing 6% Al in a base of 6 Mg/Li (weight ratio) yielded the greatest weight saving (approximately 17%) over that of 24S-T4 commercial aluminum alloy sheet when compared at a realistic, but arbitrary, performance level.

The slow-speed mechanical properties and description of the fabrication procedures for each specimen fired are presented. No simple correlation was found between the ballistic and nonballistic performance of the samples. The ballistic data are fitted by a modified Poncellet-type penetration resistance law. For the better Mg-Li alloys, it is shown that the fitted value of the parameter α in this type of law is: (1) significantly higher than that found for other fragment armors; and (2) too large to be interpreted as arising only from the presence of an inertial term in the resistance law. It is concluded that Mg-Li alloys show promise as fragment armor materials in the weight range from one to ten pounds per square foot.

PROBLEM STATUS

This is an interim report; work is continuing.

AUTHORIZATION

NRL Problem F04-02D (NA 670-022)

Work on this problem is sponsored by the Bureau of Aeronautics and is coordinated with work performed by the Battelle Memorial Institute under BuAer contract NOa(s)-9526 and NOa(s)-10026.

THE FRAGMENT PENETRATION RESISTANCE OF FOUR Mg-Li-BASED ALLOY TYPES

HISTORICAL INTRODUCTION

The earliest published work on magnesium-lithium based alloys is apparently that of Hume-Rothery, Raynor, and Butchers [1] who suggested the possibility of preparing such alloys which would exhibit age-hardening characteristics. They demonstrated their suggestion by publishing three isothermal sections of the equilibrium diagram of the Mg-Li-Ag ternary system. In discussing their diagrams, these authors noted that the β-phase Mg-Li binary material has a body-centered cubic crystal lattice. This led them to suggest that quite ductile Mg/Li based alloys could be prepared.* Apparently quite independently and possibly somewhat earlier, A. C. Loonam, while chief metallurgist for the Mathieson Chemical Corporation, was led to a similar viewpoint. As a result of this, the Mathieson Chemical Corporation initiated a program of research at the Battelle Memorial Institute designed to produce a magnesium-based alloy with improved cold-working characteristics and reduced differences in directional properties as compared with the then commercially available Mg-based alloys. This work, which has been cooperatively sponsored at Battelle by the Bureau of Aeronautics of the U. S. Navy Department since 1945, has been summarized by Jackson, Frost, Loonam, Eastwood, and Lorig. [2] Dean and Anderson [3] of the U. S. Bureau of Mines, also working independently, suggested the possibility of Mg-Li based alloys for structural applications. They noted a certain Mg-Li-Mn-Ag alloy which could be easily cold-rolled by the usual methods and was harder and stronger than the then available commercial Mg alloys. It is particularly interesting to note that these alloys of Dean and Anderson contained between 1 and 10% lithium which includes the α (hexagonal close-packed) and $\alpha + \beta$ (mixed hexagonal and body-centered cubic) fields of the binary Mg-Li alloy. While the alloys were complex it is not unreasonable to suppose that their crystal structure was essentially hexagonal close-packed or mixed. Yet they claimed high cold workability and thus implied an improvement in ductility over conventional hexagonal Mg-based alloys.

---

[1] Hume-Rothery, W., Raynor, G. V., and Butchers, E., J. Inst. Metals LXXI, 589-601, 1945

* Hofmann, W., has noted that binary Mg-Li alloys have quite low hardness. Metallkunde 28, 160-163, 1936

[2] Jackson, J. H., Frost, P. D., Loonam, A. C., Eastwood, L. W., and Lorig, C. H., J. Metals, pp. 149-168, Feb. 1949

[3] Dean, R. S., and Anderson, C. T., U. S. Patent 2,317,980, May 4, 1943, and U. S. Patent 2,376,868, May 29, 1945

The equilibrium diagram for the binary Mg-Li system has been studied by Henry and Cordiano[4] and Sal'dau and Shamraĭ,[5] but the work of Grube, von Zeppelin, and Bumm [6] has been accepted in greater detail by subsequent investigators than that of the others. Recently Shamraĭ,[7] now apparently working in Russia, has discussed the equilibrium diagram of the Al-Mg-Li ternary system. The binary diagram Mg-Li taken from Grube et al. is reproduced in Figure 1, for future reference.

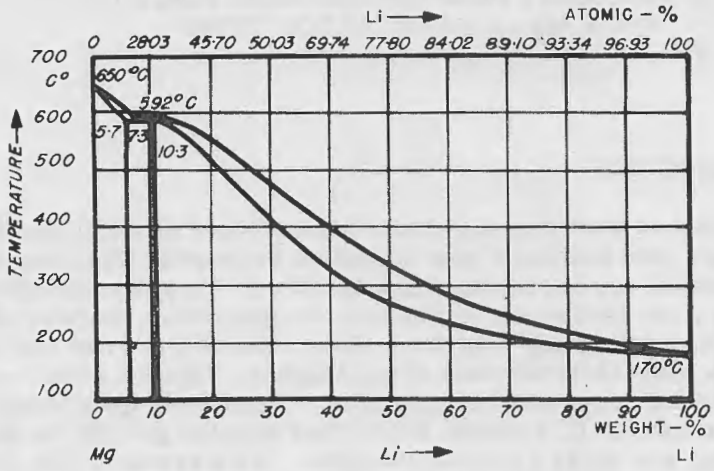

Figure 1 - Binary magnesium-lithium equilibrium diagram (after Grube)

The earliest suggestions that Mg-Li-based alloys might possess interest as armor materials resulted in preliminary ballistics tests of four plates produced by the Battelle group under BuAer contract. These materials were procured for test at the Naval Research Laboratory through the assistance of Messrs. E. N. Promisel, H. Boertzell, and C. R. LeVine of BuAer. The results of these exploratory trials were discussed by George[8] in the spring of 1947 at an ONR Symposium on Magnesium. Preliminary reports of subsequent work at this Laboratory have been made periodically.[9,10]

---

4 Henry, O. H., and Cordiano, H. V., Trans. AIME 111, 319-332, 1934

5 Sal'dau, P., and Shamraĭ, F., Z. anorg. u. allgem. Chem. 224, 388-398, 1935

6 Grube, G., von Zeppelin, H., and Bumm, H., Z. Elecktrochem. 40, 160-164, 1934

7 Shamraĭ, F., Bull. Acad. Sci. URSS Sect. of Chem. Sci., pp. 605-616, 1947; pp. 83-94, 1948

8 George, W., Report on Symposium on Magnesium sponsored by Mechanics and Materials Branch, ONR, April 22-23,1947,(A1407), pp. 15-21 (Restricted)

9 NRL Progress Reports: April 1949, p. 26; Oct. 1949, p. 25; Dec. 1949, p. 23; April 1950, p. 34

10 George, W., and Clark, J. B., "Yawed-Dart Performance of Special Mg-Li-Based Alloy Armor Plate Produced by Battelle Memorial Institute," May 17, 1949, forwarded to BuAer by NRL ltr. C3810-115/49 ks dated June 15, 1949 (Confidential)

In 1948 the Bureau of Aeronautics contract[11] at the Battelle Memorial Institute specifically included as an objective the development of a Mg-Li-based alloy armor. The 15th monthly progress report covering the activity of this endeavor during the month of November 1949 has been distributed, and the work is continuing. As the work of the Battelle group produced plates of interest, ballistic tests using the standard NRL 22-caliber 34-grain fragment-simulating yawed-dart test have been made in the Armor Materials Group of the Mechanics Division of NRL. This report discusses the results of those ballistic tests performed on all material received by NRL and discussed in Battelle progress reports 1 through 15, inclusive. Additional plates have been received, and the work is continuing, but it was considered desirable to prepare this partial summary of the experimental work completed through December 1949 at the Naval Research Laboratory.

EXPERIMENTAL TECHNIQUES

The work on the Mg-Li-based alloys at Battelle Memorial Institute has been under way for some years. Therefore in 1948 when a project was specifically designed to produce samples for light and fragment armors under sponsorship of the Materials Branch, BuAer (contract NOa(s) 9526) it was possible to make a selection of materials for an initial ballistic survey. The selection made by the Bureau and Battelle groups, at the initiation of the contract, resulted in a series of 27 plates representing essentially three Mg-Li alloy types and contained two commercial plate alloys. The results of NRL fragment-simulating 22-caliber yawed-dart tests on these materials were reported in a letter report by George and Clark in May 1949.[12]

All the ballistic tests performed to date have involved use of the standard NRL 22-caliber yawed-dart fragment-simulating projectiles. The missile is a right circular steel cylinder capped by two right cones with an included angle of 90° as shown schematically in Figure 2. The darts are fully hardened—Rockwell C 60-62.

The design parameters for this symmetrical dart are summarized in Table 1.

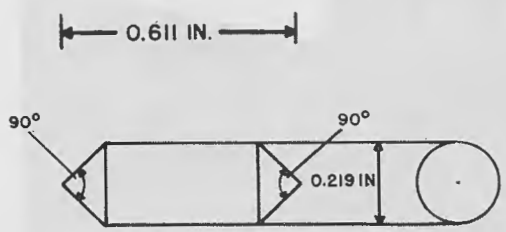

Figure 2 - Standard double ended (symmetrical) NRL 22-caliber yawed-dart fragment-simulating missile

TABLE 1

Parameters
22-Caliber Symmetrical Dart

Parameter	Value
Mass (M)	0.0798 oz (Ca. 34 grains)
Caliber (d)	0.219 in.
Length (l)	0.611 in.
Max. Presented Area (A_m)	0.110 $in.^2$
Form Factor $\frac{M}{A_m^{3/2}}$	2.18 $oz/in.^3$

Figure 3 shows a photograph of the short firing range installed within an air-conditioned laboratory room which was used in the work reported here. The attack velocities were measured with a forty-pound, five-wire suspension ballistic pendulum of a type first described by

---

11 Contract NOa(s) 9526, BuAer ltr. Aer-AE-41, Ser. 75778 dated October 14, 1948

12 George, W., and Clark, J. B., op. cit.

Irwin.[13] The gun and silencer are standard equipment. Limit velocities for the symmetrical darts are defined in the usual manner by that velocity which just accomplishes penetration. Practically, a limit velocity is obtained as the mean of two attack velocities, differing by an arbitrary amount 2ϵ, one of which just accomplishes penetration and one which does not. In order that the spread between these two velocities may be displayed in assigning a limit velocity as the mean defined above, we append to it by the sign ($\pm$) a number, ϵ, equal to half this spread. In cases where ϵ is greater than about 1% of the limit velocity it may be used as an estimate of the experimental error, in all others it merely represents the observed bracket. Often the loading is sufficiently regular to produce single rounds which just accomplish penetration, e.g.,the dart and spalls are retained by four layers of Canton gun flannel (cotton flannel), which is placed behind the armor sample. These situations are called "limit rounds" and limit velocities obtained from them are indicated by an asterisk (*) following the limit velocity (V_L).

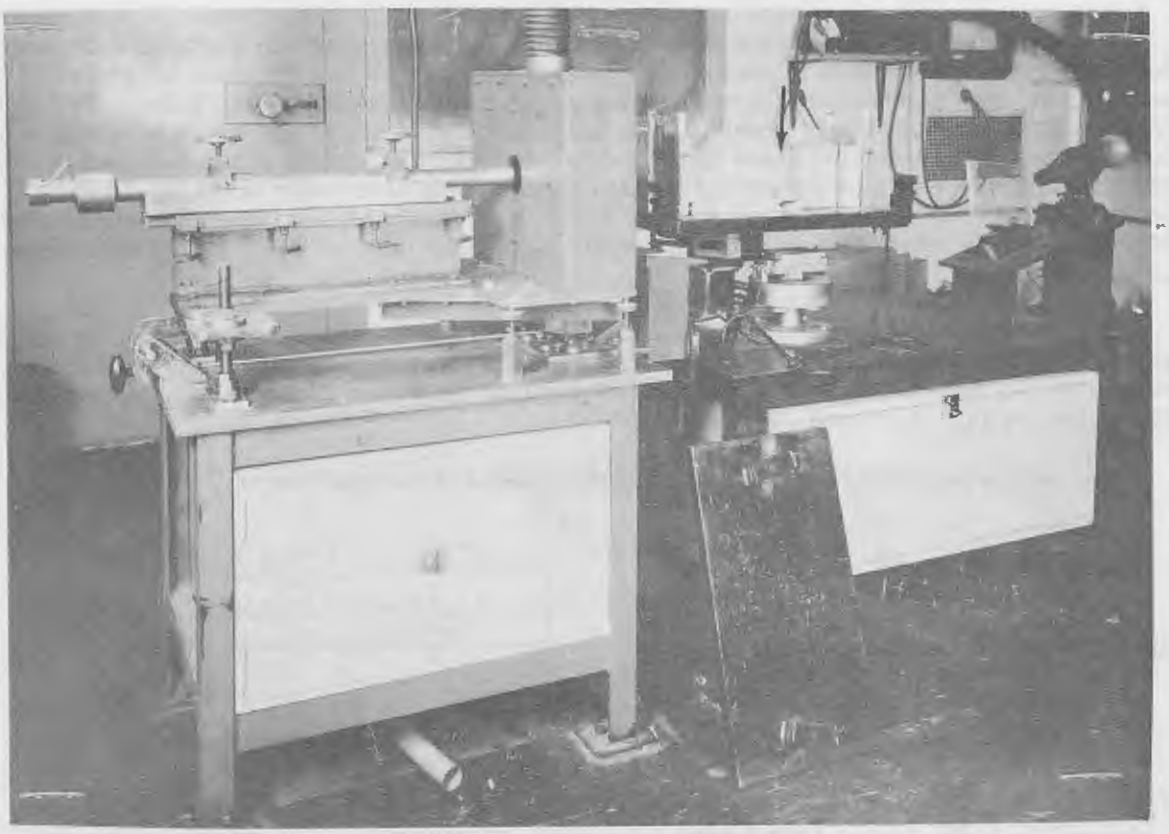

Figure 3 - NRL short-range firing facility for fragment armor evaluation. Note: The arrow ↓ denotes position of test plate in the ballistic pendulum. One side of the pendulum has been removed to expose the specimen mounting arrangement. The low-power microscope at the extreme right is used to measure dimensions of yaw-card perforation.

[13] Irwin, G. R., "Light Armor IX," NRL Report O-1778 (Restricted), Sept. 1941

The technique used to obtain yaw does not allow the exact yaw to be predicted, but the value of yaw obtained round by round was accurately measured. The limits reported here were so selected that the yaw measurements were within $\pm 5^{\circ}$ of 90°. The velocities were computed from pendulum deflections and are thought to be individually significant to within less than $\pm 1\text{-}1/2\%$.

FABRICATION

All heats were produced by the Battelle Memorial Institute group under the general direction of Dr. L. W. Eastwood. The general techniques used by this group in producing laboratory-scale melts have been described by Jackson et al.[14] Exact details are available in the fifteen monthly progress reports prepared under BuAer Contract NOa(s) 9526 which appeared between October 1948 and December 1949. The molds usually had copper bottoms and a refractory hot top, and the melts varied from about 13 pounds to about 20 pounds. Details as to fabrication are summarized in Data Tables 3, 7, and 12.

The Battelle group divided the stock from the larger heats in a characteristic fashion as indicated by the diagram in Figure 4. The smaller heats were rolled to a constant nominal thickness of 3/8 inch. Tensile coupons were taken adjacent to the various plates tested ballistically. From these, measures of tensile properties were made with one or both of two specimens; an ASTM standard sheet specimen with a 2 inch gauge length and a substandard 1/4 inch round specimen with a 1 inch gauge length. Rockwell "E" hardness and 500-kg Brinell hardness measures were made on the ballistic test plates. No chemical compositions were determined, since the intended compositions were thought to be sufficiently accurate for comparison purposes.

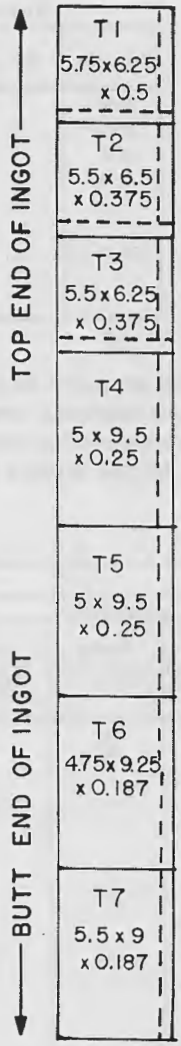

(DIMENSIONS IN INCHES)

Figure 4 - Location of ballistic test plates in forged and rolled ingots. Dotted lines indicate tensile-test specimens. Dimensions signify approximate size of plate submitted for armor test.
Note: After Frost et al., Battelle Monthly Progress Report No. 10 on "The Development of Mg-Li-Base Alloys for Armor Plate," May 1949 (Restricted)

EXPERIMENTAL RESULTS

Alloy Type I - 2 Zn, 16 Cd, 4 Ag

Four heats ranging in size from about 13 to 20 pounds were made of this alloy

14 Jackson, J. H., et al., op. cit.

type, and one modification heat, No. 2043 (2 Zn, 15 Cd, 3 Ag plus minor elements). The compositions of these five heats are summarized in Table 2 below. For convenience the density of the alloys ρ in gm/cm^3 is listed here.

TABLE 2

Nominal Compositions - Alloy Type I

Heat No.	Mg/Li	ρ	Intended Composition (%)					
			Mg	Li	Zn	Cd	Ag	Other
2040	7	1.76	68.2	9.8	2	16	4	
2045	7	1.76	68.2	9.8	2	16	4	
2211	7	1.78	68.2	9.8	2	16	4	
2394	7	1.79	68.2	9.8	2	16	4	0.15 Al
2043	6	1.65	69.6	11.6	0.25	15	3	0.16 Cu 0.1 Ba 0.1 Ni 0.05 Ca

The fabrication practice is noted in Table 3. This Table includes forging practice, rolling practice, and thermal treatments. Heats 2211 and 2394 were reheated between the principal rolling processes for short intervals (10-15 minutes) to rolling temperature. Heat 2394 was reheated in the middle of the forging operation to about 650°F before the slabbing operation.

TABLE 3

Fabrication Details - Alloy Type I

Heat No.	Forging Practice				Rolling Practice				Thermal Treatment				
	Homogenizing Treatment		Forging Temperature (°F)	Upset Reduction Ratio	Slabbing Reduction Ratio	Preheat		Rolling Temperature (°F)	Reduction Ratio	Solution		Aging	
	Temp (°F)	Time (hr)				Temp (°F)	Time (hr)			Temp (°F)	Time (hr)	Temp (°F)	Time (hr)
2040	550	5	550/450	1.3/1	4.3/1	450	16	450	3/1	600	4-6 (min) (Flattening)	~~150~~	
2045	550	16	550	1.3/1	4.3/1	450	3	500/400	3/1	(")		150	
2211 T-1	500	16	550	1.3/1	4.9/1	Not Recorded		550	2.3/1	None		150	115
2211 T-2									3.1/1			"	145
2211 T-3												"	114
2211 T-4									4.6/1			"	161
2211 T-5												"	145
2211 T-6									6.2/1			"	232
2211 T-7												"	184
2394 T-1	500	16	550/660	1.5/1	4.7/1	Not Recorded		550	2.3/1	500 (H2O Quench)	1-	150 plus 200	265 6
2394 T-2									3.0/1				
2394 T-3													
2394 T-4									4.5/1				
2394 T-5													
2394 T-6									6.0/1				
2394 T-7													
2043	500	16	550	1.3/1	4.3/1	450	3	500/400	3/1	600	4-6 (min) (Flattening)	150	

The ballistic and nonballistic properties of the plates in this class of alloy are summarized in Table 4 and the limit velocities are given in units of ft/sec in accordance with the practice described earlier. The Rockwell "E" and 500-kg Brinell hardness values are listed together with the observed longitudinal and transverse tensile properties, in units of 10^3 psi. The symbol for tensile strength used is "T.S.," yield strength "Y.S." and elongation "E". Two 3/16 inch plates of heat 2394 (T-7) were tested. One plate shattered at an attack velocity of about 1200 ft/sec, the other did not. One 1/2 inch plate from heat 2394 (T-2) also shattered on attack (2400 ft/sec). In both cases of shatter, the attack velocity appears to be near the limit velocity, but no special significance should be attached to these values.

TABLE 4

Ballistic and Nonballistic Properties - Alloy Type I

Heat No.	Thickness (in)	V_L (ft/sec)	Hardness		Longitudinal			Transverse		
					T.S.	Y.S.	E	T.S.	Y.S.	E
			"E"	BHN	(10^3 psi)		(%)	(10^3 psi)		(%)
2040 D	3/8	1865*	86.0					44.2	37.0	9 (1)
			91.5		44.3	36.6	18.5 (1)			
			94.0		41.4	36.5	17.5 (2)			
2045 D	3/8	1880±30	90.5		36.7	33.5	41.5 (1)	41.8	37.4	28 (1)
2211 B-1	1/2	2430*	94.0	82.6	45.2	35.7	20 (1)	47.8	39.0	16 (1)
2211 B-2	3/8	1935*	93.5	83.8	43.8	34.9	22 (1)	46.8	37.9	18 (1)
2211 B-3	3/8	1890±10	93.0	83.2	44.2	35.1	20 (1)	47.2	38.8	13 (1)
2211 B-4	1/4	1435*	92.0	81.3	39.7	30.1	31 (2)			
2211 B-5	1/4	1400±10	92.0	79.0	40.4	32.7	29 (2)			
2211 B-6	3/16	1205±15	92.0	79.6	38.4	30.1	35 (2)			
2211 B-7	3/16	1205*	91.0	81.3	39.7	31.1	35 (2)			
2394 T-1	1/2	2260*	98.5	94.8	45.7	38.6	9 (1)	48.7	42.4	2 (1)
2394 T-2	1/2	2160**	98.5	97.1	46.6	39.6	6 (1)	50.3	41.6	2 (1)
2394 T-3	3/8	1715*	98.5	96.7	47.5	41.2	4 (1)	49.8	44.5	1 (1)
2394 T-4	3/8	1735*	99.0	96.7	49.0	40.6	4 (1)	50.5	44.5	1 (1)
2394 T-5	1/4	1345*	99.0	94.8	46.0	37.4	3 (2)			
2394 T-6	1/4	1350*	98.5	94.8	46.4	38.5	6 (2)			
2394 T-7	3/16	1075*	98.5	93.3	46.3	38.4	8 (2)			
2394 T-7	3/16	1080*	98.5	93.3	46.3	38.4	8 (2)			
2043 E	3/8	1925*	87.5		39.9	35.9	6 (2)			
			86.0		40.6	37.0	3.5 (1)			
			87.5					43.1	39.8	4.5 (1)

* Limit velocity shot.

** Plate shattered at this velocity.

(1) Substandard tensile specimen, one-inch gage length.

(2) Standard tensile specimen, two-inch gage length.

An idea of the ballistic uniformity of heats produced on the Battelle laboratory scale can be obtained by comparing the ballistic and nonballistic properties of the 3/8 inch plates of the 7 Mg/Li, 2 Zn, 16 Cd, 4 Ag alloys. There are four heats of this alloy, three of which (2040, 2045, and 2211) were purposely treated in similar ways. One heat (2394) was subjected to a more extreme aging treatment designed to yield higher nonballistic properties. These results are summarized in Table 5.

From this table it is seen that the mean properties of the first three heats were remarkably similar to those of the individual heats; the ballistic results did not, on the average, deviate by more than about 1%. The tensile strengths and yield strength exhibited a similar

variation, and only the tensile elongation showed a large scatter (mean deviations of about 35%). It will be noted that the only nonballistic variable which would appear to correlate with the limit velocities is the hardness.* The tensile strength and hardness properties of heat 2394, purposely treated to higher values than the others, are surely significantly higher than the properties of the other heats, and similarly the ballistic results are certainly lower than those of the other heats. Comparison between heat 2394 and the other heats considered as a group, suggests that the optimum hardness for best ballistic performance (limit velocity) in alloy Type I may be somewhere between 94 and 99 Rockwell E.

TABLE 5

Reproducibility of Ballistic and Nonballistic Properties of 3/8" Plate of Alloy Type I (7 Mg/Li, 2 Zn, 16 Cd, 4 Ag)

Heat & Plate Nos.	V_L (ft/sec)	Hardness		Tensile Properties					
				Longitudinal			Transverse		
		"E"	BHN (500kg)	T.S. (10^3 psi)	Y.S. (10^3 psi)	E (%)	T.S. (10^3 psi)	Y.S. (10^3 psi)	E (%)
2040	1865*	86.0					44.2	37.0	9(1)
		91.5		44.3	36.6	18.5(1)			
2045 D	1880±30	90.5		36.7	33.5	41.5(1)	41.8	37.4	28(1)
2211 B-2	1935*	93.5	83.8	43.8	34.9	22(1)	46.8	37.9	18(1)
B-3	1890±10	93.0	83.2	44.2	35.1	20(1)	47.2	38.8	13(1)
2394 T-3	1715*	98.5	96.7	47.5	41.2	4(1)	49.8	44.5	1(1)
T-4	1735*	99.0	96.7	49.0	40.6	4(1)	50.5	44.5	1(1)
Mean (First 3 Heats)	1890 ±20	90.9 ±2.1		42.2 ±2.3	35.0 ±.8	25 ±8	45.0 ±2.0	37.8 ±.6	17 ±6

* Limit velocity shot

(1) Substandard tensile specimen, one-inch gage length.

Alloy Type II - 4 Zn, 4 Cd, 4 Ag + Minor Elements

Again arbitrarily, a second complex alloy type can be identified. For convenience, we shall term this alloy Type II. The intended composition and measured density of alloy Type II are summarized in the following Table 6. It is to be noted that heat 2212 was fabricated in a range of thicknesses (Table 7).

TABLE 6

Nominal Composition - Alloy Type II

Heat Nos.	ρ (gm/cm^3)	Mg/Li Weight Ratio	Weight (%)						
			Zn	Cd	Ag	Al	Cu	Ca	Ba
2044	1.54	6	4	4	4	0.15	0.16	0.05	0.1
2212	1.56	6	4	4	4	0.15	0.16	0.05	0.1

* The small amount of experimental data does not eliminate the possibility that this is coincidence.

TABLE 7

Fabrication Details - Alloy Type II

Heat No.	Forging Practice: Homogenizing Temp. (°F)	Homogenizing Time (hr)	Forging Temp. (°F)	Upset Reduction (Ratio)	Rolling Practice: Slabbing Reduction (Ratio)	Preheat Temp. (°F)	Preheat Time (hr)	Rolling Temp. (°F)	Reduction Ratio	Thermal Treatment: Solution Temp. (°F)	Solution Time (hr)	Aging Temp. (°F)	Aging Time (hr)
2044-B	500	16	550	1.3/1	4.3/1	450	3	500/400	3/1	450	4-6	150	
2044-E										600	(Min)	150	
2044-F										(Straightened)		150	
2044-C										700	1/2	150	300
												200	4½
2044-D										500	1	150	160
												200	4½
2212-T-1									2.3/1	NONE		150	184
2212-T-2									3.1/1	700	1/2	150	232
												200	1½*
2212-T-3										NONE		150	232
2212-T-4	500	16	550	1.5/1	4.9/1			550	4.6/1	700	1/2	150	232
										NONE		200	1½*
2212-T-5												150	161
2212-T-6									6.2/1	700	1/2	150	232
2212-T-7										NONE		200	1½*
												150	184

* This treatment followed the 150°F aging

In Table 8 we summarize the ballistic and nonballistic properties of the two heats of alloy Type II. Certain of the entries here are worth noting. In particular, it is possible to argue that the data for the 3/8 inch plate is internally consistent, in spite of its apparent inconsistencies. We start by noting that, in essence, two types of fabrication procedure were used, one a solution heat treatment of 700°F and the second a solution heat treatment of about 500°F (rolling temperature); in one case the rolling temperature, in a second a bona fide thermal treatment following rolling. Plates 2212 T-2 and T-3 indicate that the higher solution temperature is accompanied by lower limit velocities. Now 2044-B again shows a higher* performance than 2044-C (700° solution temperature) which is entirely consistent with 2212 T-3 and 2212 T-2 respectively. (The hardness of 2044-B is slightly lower than 2212 T-3 which probably accounts for the slightly smaller difference in the former heats.) It would appear that plate 2044-D should have a higher limit in view of the 500° F solution temperature used. However, we note (Table 8) that this plate was fired with the dart axis oriented at right angles to the direction of rolling, while the other plates had the dart axis parallel to the direction of rolling. A dart oriented at right angles to the direction of rolling weights preferentially the longitudinal properties, while an orientation parallel to the rolling direction will yield performance weighted to the transverse mechanical properties. (It is to be noted from the nonballisitc properties measured on 2212 T-1 and 2212 T-3 that this lower heat treatment produces, in general, higher transverse strength properties than longitudinal while the 700° temperature appears to tend to produce more nearly equal properties.) It would appear then, that the 3/8 inch plate data from both heat 2044 and heat 2212 is qualitatively quite constant, and further demonstrates the reproducibility and reliability of the results.

Alloy Type III - α (Mg-Li) and $\alpha + \beta$ (Mg-Li)

As the third alloy type studied in this work, it is convenient to group together those alloys containing grains of the α phase (hexagonal close-packed crystal structure). The

* The difference in V_L for these plates, 35 ft/sec, is, however, just barely experimentally significant.

alloys are chemically much simpler than those grouped in Types I and II. Their nominal compositions are listed in Table 9.

TABLE 8

Ballistic and Nonballistic Properties - Alloy Type II

Heat No.		Nominal Thickness (in)	V_L ft/sec	Hardness		Longitudinal			Transverse		
				"E"	BHN	T.S. (10^3 psi)	Y.S. (10^3 psi)	E (%)	T.S. (10^3 psi)	Y.S. (10^3 psi)	E (%)
2044	B	3/8	(∥) 1859±20	88.5		39.4	34.9	18.5(2)			
	E	3/8		88.5		39.1	35.1	18 (2)			
	F	3/8		79.5		29.4	25.8	38			
	C	3/8	(∥) 1825±10	90.5							
			(⊥) 1770*	93		46.0	33.7	2 (1)			
				93.5		46.4	44.2	(1)			
	D	3/8	(⊥) 1765±15	89.0							
				88.0		39.2	35.5	17 (1)			
2212	T-1	1/2	2455±10	90.0	79.0	38.8	34.3	24 (1)	41.1	36.8	13(1)
	T-2	3/8	1825*	95.5	85.1	40.8	36.8	9 (1)	40.8	37.2	2(1)
	T-3	3/8	1915±10	90	78.4	37.2	30.2	22 (1)	40.2	33.5	14(1)
	T-4	1/4	1365±10	92.5	78.4	38.2	33.4	13 (2)			
	T-5	1/4	1395*	90.0	77.9	37.9	33.3	21 (2)			
	T-6	3/16	1170*	91.5	79.6	38.1	35.1	11 (2)			
	T-7	3/16	1175*	90.0	74.6	37.3	34.8	27 (2)			

* Limit velocity shot

(∥) Refers to orientation where the axis of the test dart is parallel to the rolling direction.

(⊥) Refers to orientation where the axis of the test dart is perpendicular to the rolling direction.

(1) Substandard tensile specimen, one-inch gage length.

(2) Standard tensile specimen, two-inch gage length.

TABLE 9

Nominal Compositions - Alloy Type III

Heat No.	Mg/Li Weight Ratio	Zn	Ag	Al	Mn	ρ (gm/cm^3)
2048	13.3	4	6			1.69*
2047	24			4		1.64
FS-1h (Dow)		1		3	0.3	1.75
FS-1r (Dow)		1		3	0.3	1.75

* Mixed microstructure, all others completely α-phase (HCP).

The fabrication practice of heats 2047 and 2048 was quite similar to the heats described in alloy Types I and II. Since there did not seem to be any particular point in displaying the details, the interested reader is referred to the original reports on the subject.[15] All plates in this alloy type were 3/8 inch thick. Typical ballistic properties obtained are summarized in Table 10. While the limits obtained on heat 2047 and the FS-1r Dow plate are not as precise as might be desired, it seems quite probable that the mixed structure of heat 2048 ($\alpha + \beta$) possesses a slightly higher penetration resistance than that of the completely α structures. It may be, however, that this is quite accidental since there are quite important chemical differences between the heats of this group.

[15] Frost, P. D., et al., Monthly Progress Report No. 8 on Development of Mg-Li-Based Alloys for Armor Plate, Battelle Memorial Institute (Restricted), June 1949

TABLE 10

Ballistic and Nonballistic Properties - Alloy Type III										
Heat No.	Nominal Thickness (in)	V_L (ft/sec)	Hardness		Longitudinal			Transverse		
					T.S.	Y.S.	E	T.S.	Y.S.	E
			"E"	BHN	(10^3 psi)		(%)	(10^3 psi)		(%)
2048 B	3/8	1835±25	82		34.8	27.4	32.5(2)			
			82		34.9	27.8	32.5(2)			
			79					36.2	25.9	31(1)
			82.5					36.3	26.1	28(1)
			82		36.5	28.4	25(1)			
			80		36.8	28.4	32(1)			
2047 B	3/8	1750±80	78		34.5	21.5	20(2)			
			78		31.3	21.0	7(2)			
			75.5		35.5	22.6	22(1)			
			75.5		35.2	23.1	22(1)			
			73					33.8	22.9	26(1)
			73					34.2	22.9	26(1)
FS-1h Dow	3/8	1740±25	82	54.0	39.2	27.1	19(2)			
FS-1r Dow	3/8	1780±65	82		37.2		20(2)			

(1) Substandard tensile specimen, one-inch gage length.
(2) Stardand tensile specimen, two-inch gage length

Alloy Type IV - Simple Compositions, β (Mg-Li)

TABLE 11

Nominal Composition - Alloy Types IV			
Heat No.	Mg/Li Weight Ratio	Al	ρ (gm/cm^3)
2391	8.1		1.48
2213	6	6	1.44

The remaining two heats studied to date are grouped together in alloy Type IV. These are both simple alloys: one a binary Mg-Li, β phase, the other a ternary Mg-Li-Al alloy. Their chemical compositions are given in Table 11 and the fabrication procedures for these alloys are outlined in Table 12. The ballistic and nonballistic properties of the heats are given in Table 13. It will be noted that the harder, and hence the stronger, alloy (heat 2213) yielded higher limit velocities, thickness for thickness, at the 1/2 inch and 3/8 inch level. The situation is reversed in the thinner plates (1/4 inch and 3/16 inch). Heat 2391 shows about a 12% increase in hardness from the 1/2 inch plate to the 3/16 inch plate. It is not unlikely, therefore, that if larger ingots of the binary alloy were made so that 1/2 inch plate could be given more mechanical working, the limit velocities might approach or exceed those of the more complex 6 Mg/Li, 6 Al alloy (heat 2213).

TABLE 12

Fabrication Details - Alloy Types IV													
Heat No.	Forging Practice				Rolling Practice					Thermal Treatment			
	Homogenizing		Forging	Upset	Slabbing	Preheat		Rolling	Reduction	Solution		Aging	
	Temp. (°F)	Time (hr)	Temp. (°F)	Reduction (Ratio)	Reduction (Ratio)	Temp. (°F)	Time (hr)	Temp. (°F)	Ratio	Temp. (°F)	Time (hr)	Temp. (°F)	Time (hr)
2391 T-1	550	16	550	1.6/1	4.4/1	—	—	550	2.3/1	NONE		NONE	
2391 T-2									3.0/1				
2391 T-3									4.5/1				
2391 T-4									6.0/1				
2391 T-5													
2391 T-6													
2391 T-7													
2391 T-8													
2213 T-1	700	16	650	1.4/1	4.7/1	—	—	550	2.3/1	500	1	200	3/4
2213 T-2									3.1/1	700	1½	200	3¾
2213 T-3										500	1	200	3/4
2213 T-4									4.6/1	700	1/2	200	3¾
2213 T-5										500	3/4	200	1/2
2213 T-6									6.2/1	700	1/2	200	4
2213 T-7										500	3/4	200	1/2

TABLE 13

Ballistic and Nonballistic Properties - Alloy Types IV (Simple β Phase)

Heat No.		Nominal Thickness (in)	V_L (ft/sec)	Hardness		Longitudinal			Transverse		
						T.S.	Y.S.	E	T.S.	Y.S.	E
				"E"	BHN	(10^3 psi)		(%)	(10^3 psi)		(%)
2391	T-1	1/2	2175±30	44	36.3	17.1	14.1	43(1)	18.2	15.3	37(1)
	T-2	1/2	2250±20	44.5	35.5	17.7	14.3	39(1)	18.1	15.2	37(1)
	T-3	3/8	1925±25	46.5	36.2	17.9	14.1	37(1)	18.1	15.1	51(1)
	T-4	3/8	1870±10	46	36.2	17.6	14.2	42(1)	18.2	15.4	37(1)
	T-5	1/4	1530±30	49.5	37.2	17.8	14.8	53(2)			
	T-6	1/4	1480±20	49.5	37.5	18.1	15.4	66(2)			
	T-7	3/16	1295±10	51.0	37.3	18.7	15.8	57(2)			
	T-8	3/16	1325±10	50.5	37.2	18.8	14.8	51(2)			
2213	T-1	1/2	2565±10	92.0	79.6	36.3		17(1)	39.6	36.1	12(1)
	T-2	3/8	2000*	88.5	72	35.6	28.8	23(1)	37.9	32.0	19(1)
	T-3	3/8	1975±10	92	77.9	40.8	37.0	10(1)	42.3	38.4	10(1)
	T-4	1/4	1325*	88	73	35.6	31.3	20(2)			
	T-5	1/4	1355±25	90.5	74.6	37.5	36.5	19.5(2)			
	T-6	3/16	1170±10	92	77.9	Cracked under test					
	T-7	3/16	1200±25	87.5	74.1	37.6	36.0	18(2)			

* Limit velocity shot.

(1) Substandard tensile specimen, one-inch gage length.

(2) Standard tensile specimen, two-inch gage length.

THE PENETRATION OF ARMOR - EFFECTS OF ARMOR DENSITY, MECHANICAL STRENGTH, AND BALLISTIC BRITTLENESS ON FRAGMENT PENETRATION RESISTANCE

From points within an armor, its penetration may be regarded as accomplished against certain resisting pressures P. Just as the work done in compressing a volume V of a gas by an amount dV is PdV; so also may one regard the work in penetrating armor by a volume $d\Omega$ as $Pd\Omega$. From this viewpoint, the pressures P constitute a measure of the resistance offered by the armor to the penetration by the attacking missile. The volume Ω is estimated in terms of coordinates fixed originally in the undisturbed plate material. The resistance pressure P can be expressed as a function of the distance, Z, from the front face in the undisturbed plate. After penetration of a plate of armor by a missile with velocity V_L which attacks with just sufficient energy to accomplish the penetration, one usually finds that portions of the plate material at the front and back of the armor have been thrown clear. These we shall term spall particles or just simply spalls. A cross-section of such a typical plate is shown diagrammatically in Figure 5. Penetration is accompanied by a general distortion of planes fixed originally in the plate before penetration. This distortion is shown schematically in Figure 5a, where the dashed lines show the intersection of the distorted planes (ξ planes) with the section. Figure 5b shows the same intersections if one were to remove the warping which accompanies the penetration (Z planes). The distance Z is measured from zero at the front of the plate to Z = e, the armor thickness at the back of the plate.

In general during a given penetration, the time average of P acting across a laminar section between Z and Z + dZ may be regarded* as a concave downward function of Z, as shown schematically in Figure 6. The successive layers of plate material counted from the front face of the armor contribute successively more to the time average resistant

* The general case shown in Figure 6 allows for many relative maxima.

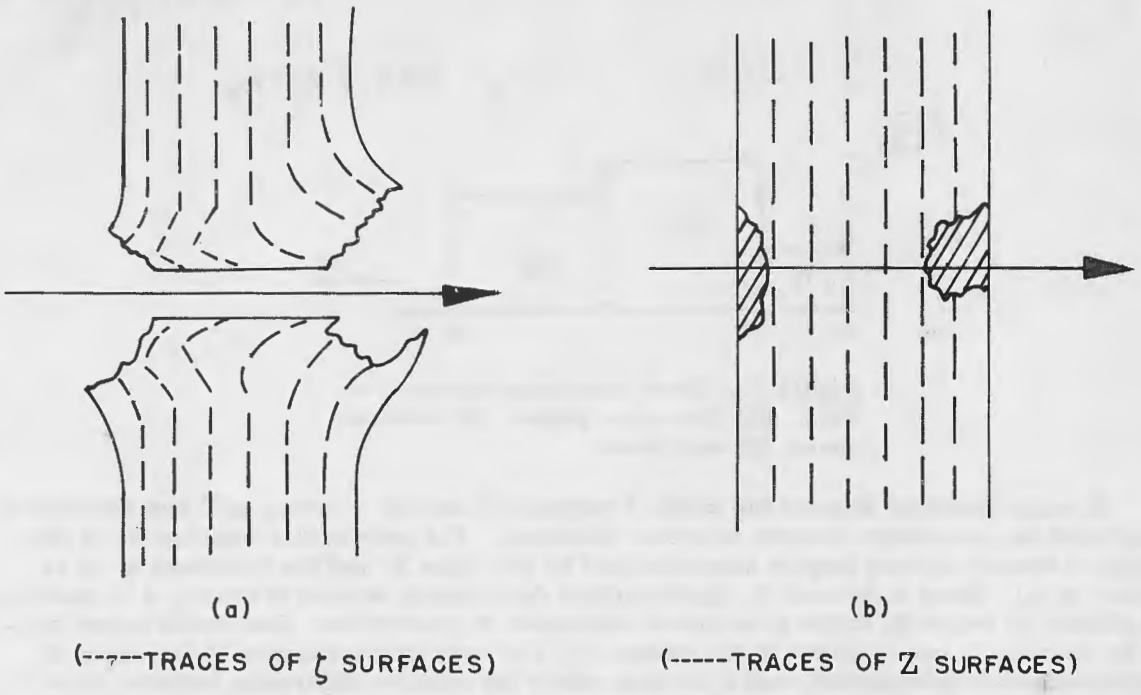

Figure 5 - Idealized cross-sections of penetration: (a) as observed with the distortion resulting from penetration and (b) referred to Z planes originally fixed in the armor

pressure P, until some maximum* time average pressure is reached which acts across planes located in the central sections of the original plate. Pressures for greater Z decrease to zero as the rear face of the armor is approached. In general, the lower values of P(Z) are anticipated in regions near the plate faces. The occurrence of face spalling in these regions demonstrates the reduction in P(Z) associated with the face surface. In this case we may use face surface effects as a measure of ballistic brittleness. Delamination in the center regions similarly reduces the high resistant pressures which characterize the central regions of the plate.

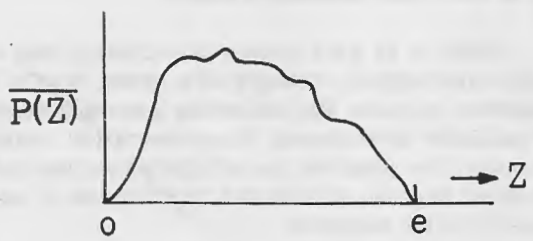

Figure 6 - Time average pressure $\overline{P(Z)}$ vs. Z. Distance through the plate, Z, is measured in the undisturbed plate.

The general case just described and illustrated in Figure 5 may be crudely approximated by a three-step P(Z) function as illustrated in Figure 7. By referring to Figure 5b we see that a region (1) can be defined which includes all Z values intersecting the region connected with face spalling. Similarly a region (3) may be selected which includes all Z values associated with back spalling. Region (2) refers to those portions of the plate in which the deformation is to be regarded as free from the complications of fracturing.

* A generalization from experimental results obtained from projectile penetrations by G. R. Irwin, op. cit.

[redacted]

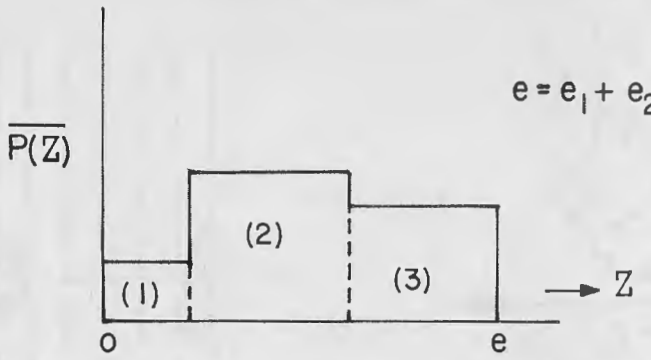

Figure 7 - Three-step approximation to $\overline{P(Z)}$. (1) Entrance phase, (2) central phase, (3) exit phase

In many practical armors the width of regions (1) and (3) in terms of Z are essentially unaltered by reasonable changes in armor thickness. The penetration resistance* of this class of armors is thus largely characterized by the value P_2 and the thickness e_2 (e is linear in e_2). Since in general P_2 characterizes deformation without fracture, it is plausible to attempt to relate P_2 to the slow-speed resistance to penetration. One would expect this to be possible in one of either of two cases: (1) The case where changes in the speed of deformation are unimportant, and (2) the case where the relative difference between slow and rapid deformation is a slowly varying function of changes in the speed of rapid deformation. In these cases, we should expect then, that P_2 would be characterized by the results of slow-speed indentation hardness tests such as the Brinell hardness. The deeper the indent used in such tests, the more closely we would expect the result to reflect the quantity P_2 in the cases indicated above.

Since it is well known empirically that deep indentation hardness numbers and the ultimate mechanical strength of a given type of metal are approximately linearly related, it is possible to make the following generalization: as a first approximation, for equal degrees of ballistic brittleness, the penetration resistance of two equal thickness materials will be greater, the greater the ultimate mechanical strength of the armor. The qualification as to equal degree of ballistic brittleness is necessary, and requires the extent of regions (1) and (3) to be constant.

A second generalization is possible, which can also be regarded as a first-order approximation. It is immediately obvious from the description of the preceding paragraphs. For equal strengths, the greater the ballistic brittleness, (i.e., the greater the extent of regions (1) and (3) either together or singly) the lower the penetration resistance.

An equally obvious third generalization is possible involving a consideration of density changes. We assume the extent (geometrical widths) of the entrance and exit regions of the plate is constant (equal ballistic brittleness in those cases where the entrance and exit regions are controlled by fracturing phenomena). In this case for materials of equal strength, the ballistic performance will be the higher the lower the plate density. There is evidence,

* Penetration resistance in general refers to the energy to penetrate a given volume of plate. It is proportional to the kinetic energy of a missile attacking at limit velocity. The limit velocity is measured as the mean of two attack velocities., one which penetrates with residual velocity of an arbitrary amount 2ϵ and one which just fails penetration by a like amount.

as noted above, that the "free surface" effects are in fact confined to a nearly constant portion of the plate thickness and that it is the central region which increases with plate thickness. [16]

By increased ballistic brittleness one means an increased extent of e_1, and/or e_3, i.e., an increased extent in the entrance and/or exit phases of the penetration process. For a given P_2 it is easily seen that the energy absorbed in the central region is decreased in proportion to the amount by which the widths of the entrance and exit phases in Z space are increased.

The three-stage approximation to the penetration event has been useful in introducing a qualitative discussion of the following simple alterations in the penetration resistance.

1. Effect of increasing penetration resistance by increasing armor strength at constant armor thickness (and weight).

2. Effect of increasing penetration resistance by reducing ballistic brittleness (decreased first and third stages of the approximate force law).

3. Effect of increasing penetration resistance by decreasing the armor density at constant armor weight and strength.

It should be noted that increasing strength (effect 1) must not be accompanied by increased ballistic brittleness (effect 2) if the former is to result in a maximum improvement. Unfortunately, it appears that many mechanical and metallurgical procedures, which would otherwise increase armor strength, simultaneously increase the ballistic brittleness.

DEMONSTRATIONS OF THE RESULTS OF THE PREVIOUS SECTION

Before demonstration of the above ideas, it is necessary to develop further the concepts of strength and free surface introduced above. It is well known, especially as previously noted, that the ultimate tensile strength of steel alloys is nearly a linear function of the indentation (Brinell) hardness. A similar relation appears to exist for Mg-Li alloys, as shown in Figure 8. In general there appears to be a different relation between tensile strength and hardness for the β-phase alloys and that for the α-phase alloys. The mixed microstructures appear to be intermediate cases.

The simple binary alloy (alloy Type IV) provides a visual demonstration of the usefulness of the concept of the free surface regions (Regions (1) and (3), Figure 7) of the armor. These alloys are of nearly equal density, hence one may compare the entrance and exit deformations between the two alloys at equal thicknesses. Figures 9a and 9b show sections through 1/2 and 3/8 inch plates, respectively, of the binary alloy (heat 2391) when attacked by the dart at velocities slightly below their respective limit velocities (about 2500 and 2100 ft/sec respectively). These sections show quite comparable front surface coronet formations and rear surface bulges. One can qualitatively interpret these photographs as indicating the constancy of the free surface effects as the plate thickness is varied. Figure 10 refers to the 3/8 inch plate and shows a normal view of the face coronets and flow markings (a) and oblique views of the rear bulge (b) and (c). Figure 11 shows similar views for the 1/2 inch plate. (The last two figures were taken before sectioning the plate.)

---

16 Irwin, G. R., and Kinzer, G. D., Light Armor VI, NRL Report O-1591 (Unclassified), Feb. 1940

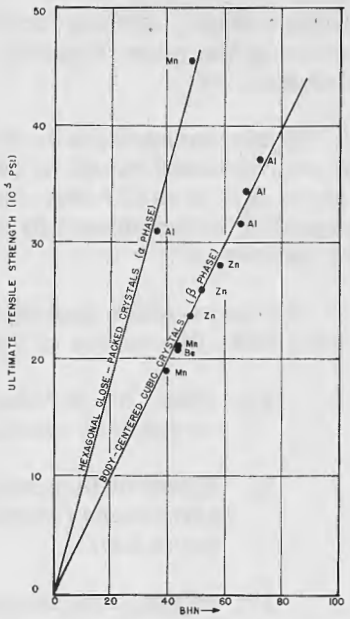

Figure 8 - Tensile strength vs. Brinell hardness, Mg-Li-based alloys extruded bar stock (Mathieson Chemical Corp.) (After Jackson et al., op. cit.)

(a) One-half-inch plate

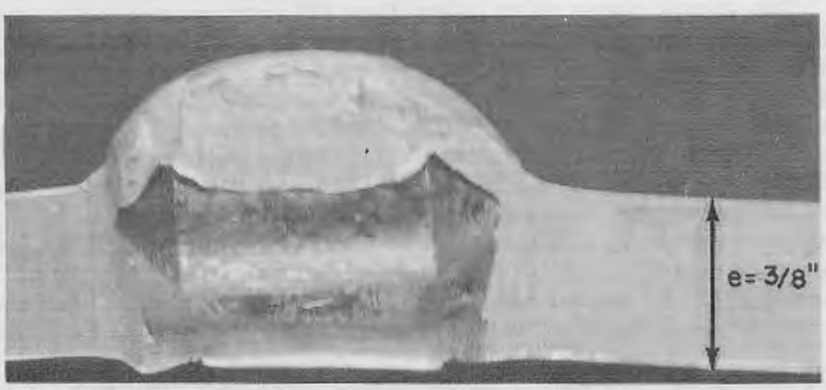

(b) Three-eighths-inch plate

Figure 9 - Sections of fired plates (heat No. 2391). Attack velocity is slightly less than limit velocity of plate, in each case.

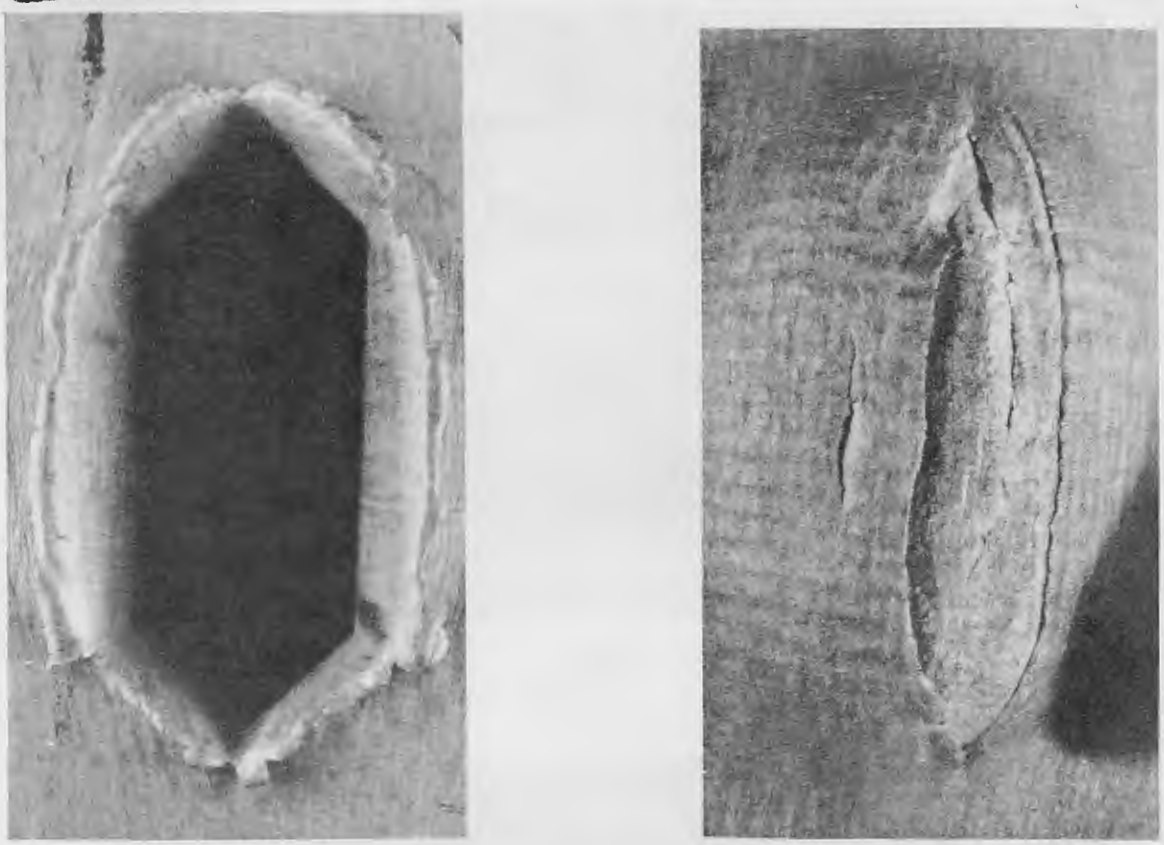

(a) Front face (b) Rear face

Figure 10 - Faces of 3/8-inch plate of binary Mg-Li alloy (heat No. 2391) after partial penetration by symmetrical yawed dart

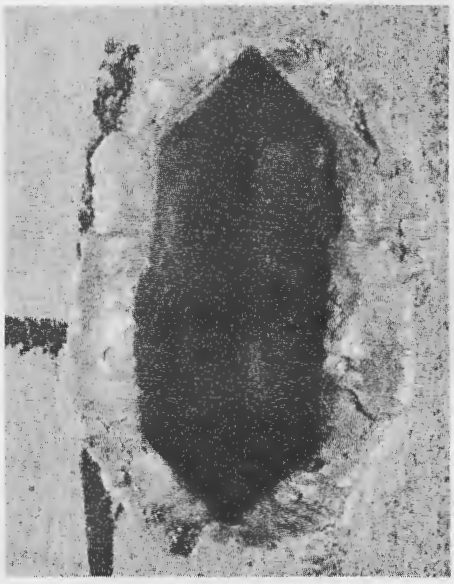

Figure 11(a) - Front view of partial penetration into 1/2-inch plate of heat No. 2391. Note recovery of plate material around the sides of the retained dart.

11 (b)

11 (c)

Figures 11(b) and (c) - Oblique views of bulge at rear of 1/2-inch plate from binary alloy (heat No. 2391)

The first effect discussed in the preceding section may be demonstrated from the ballistic data prescribed in preceding section of this report. The bulge deformation evidenced by the binary alloy (heat 2391) is quite similar to that of the stronger 6 Mg/Li, 6 Al alloy (heat 2213). The free surface similarity of this heat (2213) to the ballistically ductile binary alloy (2391) is evident by comparing Figures 10 and 11 with Figure 12. The greater performance of 2213 over 2391 is to be interpreted as due to a higher central resistant pressure P_2.* Density differences make this type of analysis complex when one attempts to explain the performance of the other alloy types.

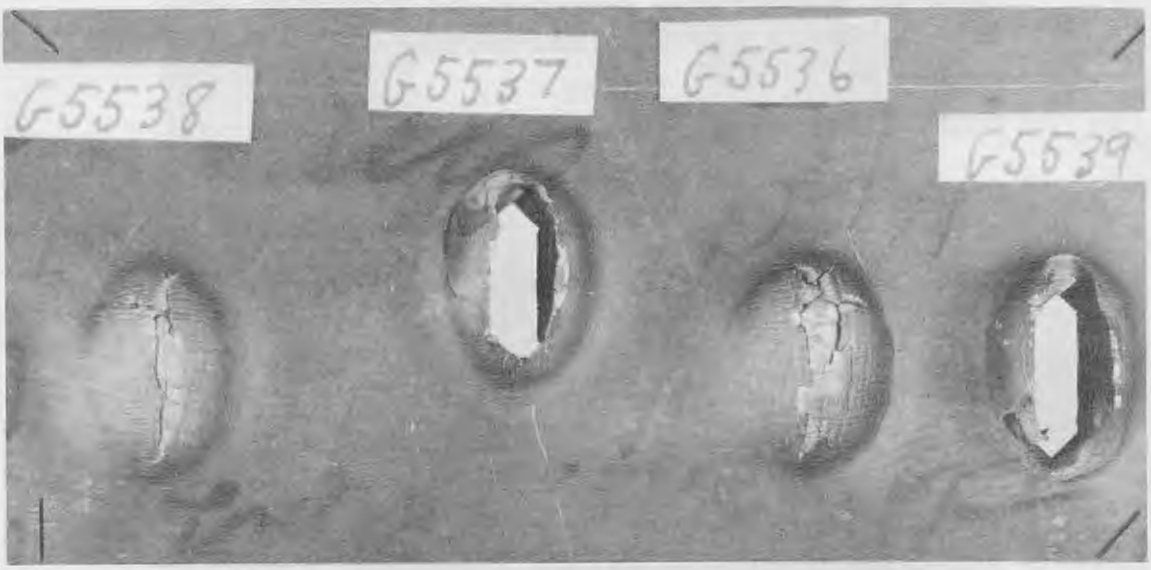

Figure 12 - Rear face damage in 3/8-inch plate of heat 2213, alloy Type IV (6 Mg/Li - 6 Al). This alloy is ballistically stronger than those shown in Figures 10 and 11 (binary Mg/Li). Note the tendency to form circumferential cracks.

The second effect discussed in the preceding section finds an obvious demonstration by referring to Figures 13 (a) and (b) taken from 3/8-inch plates of heats 2211 and 2394 respectively (alloy Type I). The difference in limit velocity represented here is about 150 ft/sec and is satisfactorily explained qualitatively in terms of a free-surface effect suggested by the differences in the appearances of the plate damage. The relative differences in the appearance of the damage is qualitatively similar for all thickness levels studied; the damage, of course, changes with thickness. Figure 14 shows an enlarged view of the rear of plate T4, heat 2394.

An illustration of the density effect (3 of the preceding section) is demonstrated clearly by the results with plates 2213 T-2 and T-3 and the plates 2212 T-3 and T-4 (Tables 13 and 8). The latter materials have a density of 1.56 while the former have a density of 1.44, about a 10% difference. At the weight level of 2213 T-2 and 2213 T-3 ($V \approx 2200$ ft/sec) we may seek the performance of a plate of equal weight of heat 2212 having a thickness of about 0.346 inch; or about 1/5 the range between 2212 T-4 and 2215 T-5. If we interpolate the limit velocities of these plates to obtain an approximate

* The thinner plate limit velocities would appear to negate this conclusion, but the difference in this case clearly are not experimentally significant.

(a) Rear face 3/8-inch-plate, heat no. 2211

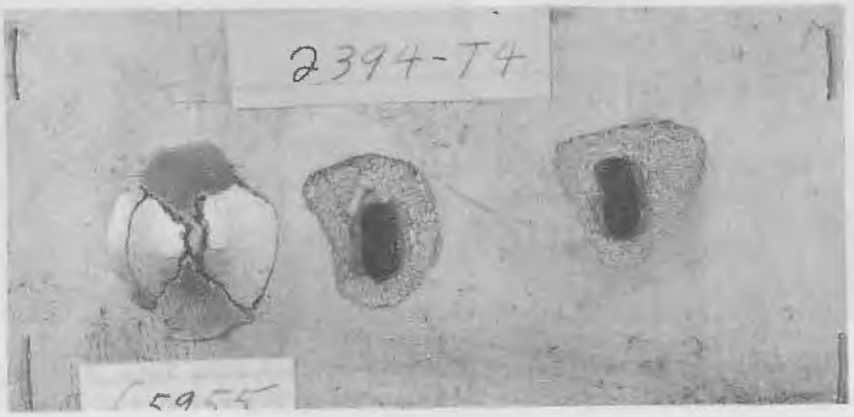

(b) Rear face 3/8-inch-plate, heat no. 2394

Figure 13 - Extent of free surface, alloy Type I. (a) Nominal free surface, (b) extended free surface effect associated with greatly increased spall formation, due probably, to increased degree of precipitation.

limit to compare with 2213 T-2, we obtain a value of about 2000 ft/sec, a value 10% lower than that representative of the lower density heat 2213. The strengths (hardnesses) of the plates used for this demonstration are quite comparable (BHN 78-79).

VARIATIONS OF PERFORMANCE WITH ARMOR THICKNESS - THE INERTIAL CORRECTION TO THE CENTRAL RESISTANT PRESSURE

The simple earlier considerations lead to the prediction that, for given free surface effects, the energy absorption will vary linearly with e_2 or the armor thickness e (which is equal to it within the additive "free surface" constant $e_1 + e_3$). One would thus from this viewpoint expect that plots of the limit energy, or more simply the square of the limit velocity vs. the armor thickness, to be approximately linear with a positive intercept on the thickness axis.

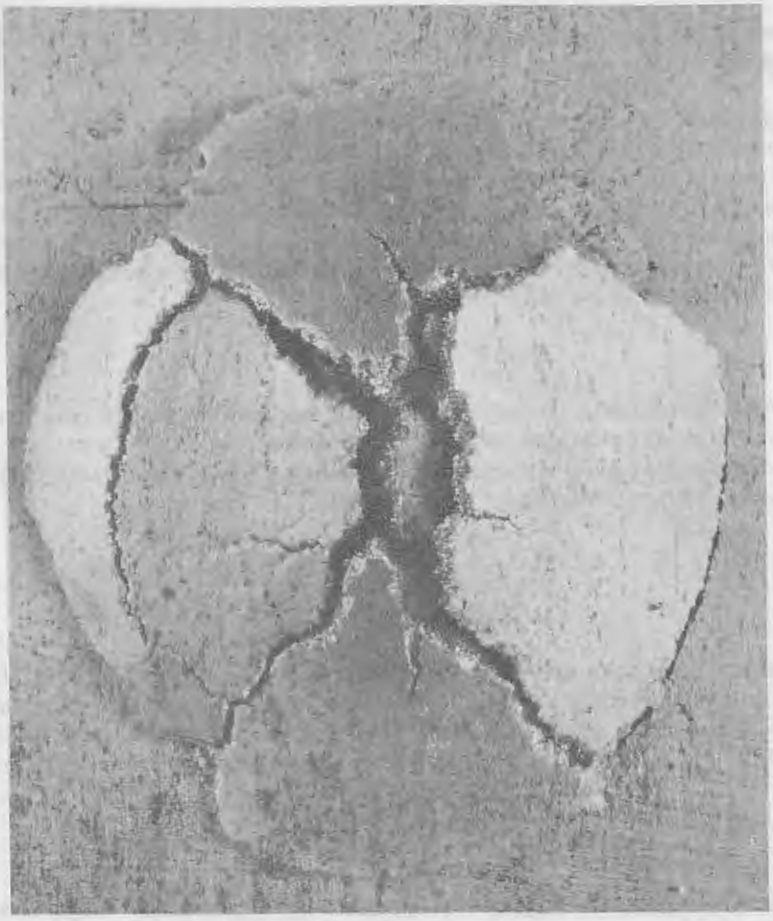

Figure 14 - Incipient spall formation in rear. Free surface, 3/8-inch plate, heat 2394. Compare this deformation with that shown in the binary alloy (Figures 10 and 11).

If one is concerned with a narrow range of armor thicknesses, the type of approximation to the forces resisting penetration referred to above is certainly adequate for organizing experimental data. On the other hand, if one has a wider range of armor thickness (say greater than about a two-fold range) such a representation is inadequate to account for the curvature (concave toward the axis of limit energy) evident in most experimental plots of limit energy vs. thickness.

An a priori explanation for this observed curvature in fragment penetration data is found in the additional resistance arising from the inertia of the plate material which must be moved out of the path of the penetrating missile. Such inertial resistance was apparently first described by Poncelet [17] over a hundred years ago. This mechansim has been used as

[17] Poncelet, Introduction à la Mécanique Industrielle Brussels, 1839, p. 619 (early edition only). See H. P. Robertson, "Terminal Ballistics," NDRC Preliminary Report, Jan. 1941

δx in time δt, the change in momentum δM of plate material $\delta \Omega$ penetrated will be,

$$\frac{\delta M}{\delta t} = \rho \frac{\delta \Omega}{\delta t} = \rho A_n \frac{\delta x}{\delta t} V = \rho A_n V^2.$$

Comparing this with the second term in (1) we see that if we interpret the latter as an inertial resistance, $\alpha \leq 2$. Probably a better estimate of an upper limit to α is obtained if we replace V in (5) by V/2, the mean velocity the element of mass $\rho \delta \Omega$ attains in time δt in passing from V = 0 to V = V. In this case, it would appear that a value of $\alpha \approx 1$ would represent an upper limit. George[20] has shown that the fragment penetration data obtained with spheres and yawed darts could be represented by (1) with values of α which were fitted within ordinary experimental errors by

$$\alpha = 1/3,$$

the value of P varying with the strength of the material.

Values of $\overline{P} = \rho_S P/\rho$ and α were fitted to some of the data reported in the previous sections of this report. The values obtained are listed in Table 14 below. It will be noted that heat 2391 gave a value near that of 1/3 found previously for many other materials. The other heats yielded values α which are considerably greater. One is led to the conclusion, then, that these high values of α fitting the data of the better Mg-Li alloys studied here indicate that an interpretation of α as an inertial coefficient cannot be maintained.[21]

TABLE 14

Poncelet Parameters for Mg-Li Alloys

Heat No.	$\overline{P}$ (10^3 psi)	α
2211	242	1.5
2212	259	1.9
2213	248	2.7
2391	384	.4
2394	265	1.3

The degree with which formula (1) represents fragment limit velocities for selected Mg-Li alloys is indicated in Figures 15 through 19. It is to be noted that these plots suggest that X_0, the free surface parameter, is never large for these materials.

PROBABLE COMPARISON OF FRAGMENT PENETRATION RESISTANCE OF Mg-Li ALLOYS WITH OTHER FRAGMENT ARMORS

The Mg-Li alloys made to date have been laboratory-scale heats. Such heats can show, and often have shown in the past, abnormal quantitative penetration resistance characteristics. Any quantitative comparisons between such heats and samples drawn from fragment armor production must be prefaced with a statement of caution concerning the quantitative relations such a comparison displays. It is to be hoped that within the near future, a reasonable quantity of Mg-Li alloy sheet and plate will be produced by a commercial fabricator so that a more precise evaluation can be made of the armor character of these alloys relative to standard metal fragment armors, such as 24S-T4 aluminum alloy.

---

20 George, W., op. cit. (Ref. 18)

21 NRL Progress Report, April 1950, p. 34. (The $\overline{P}$ and α values reported in this reference were in error and have been corrected in this report.)

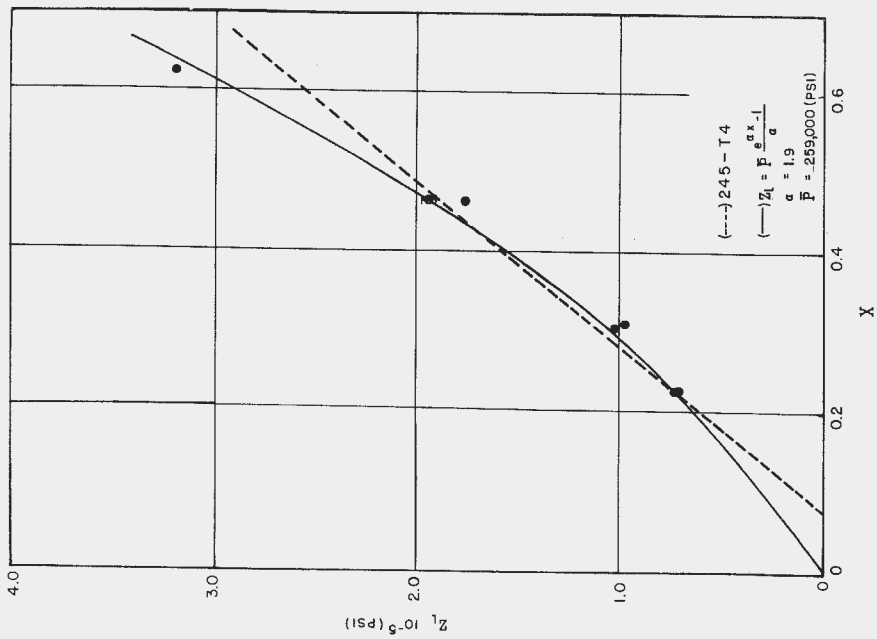

Figure 16 - Alloy Type II, heat No. 2212, Z_L vs. X

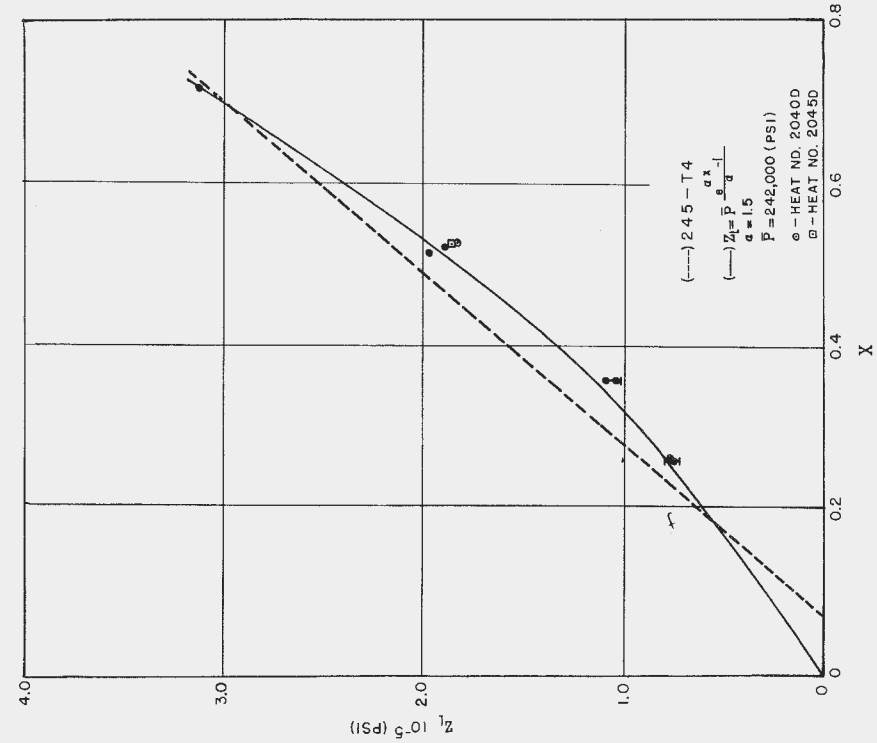

Figure 15 - Alloy Type I, heat No. 2211, Z_L vs. X

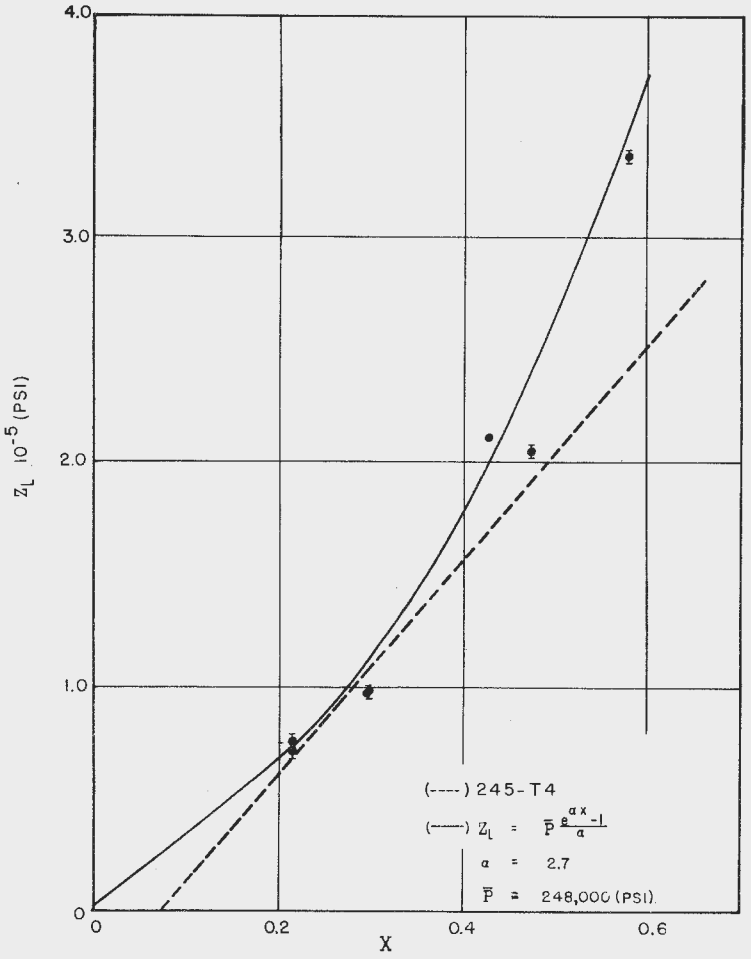

Figure 17 - Alloy Type IV, heat No. 2213, Z_L vs. X

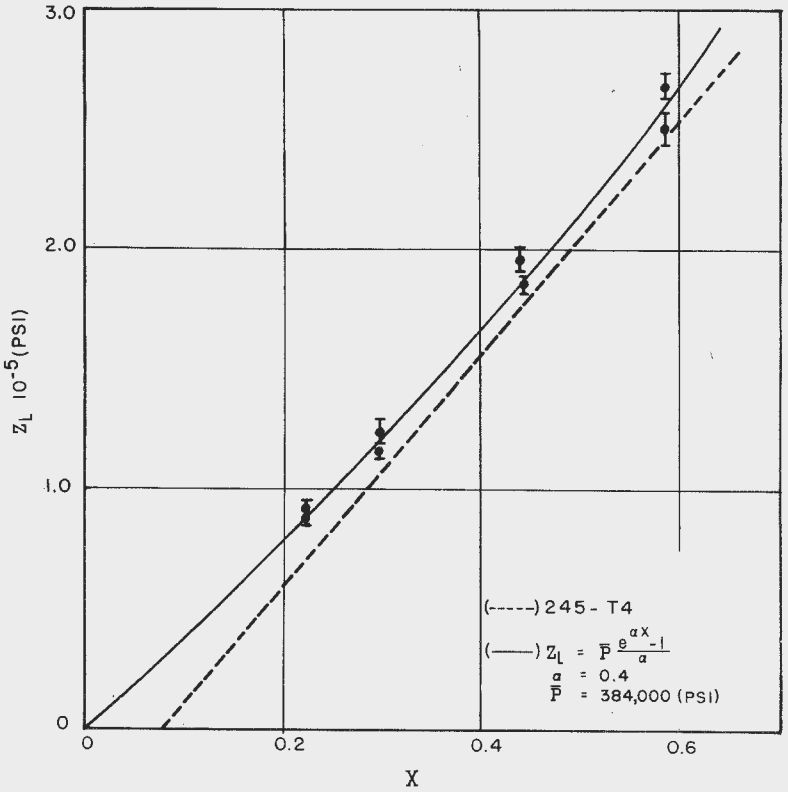

Figure 18 - Alloy Type IV, heat No. 2391, Z_L vs. X

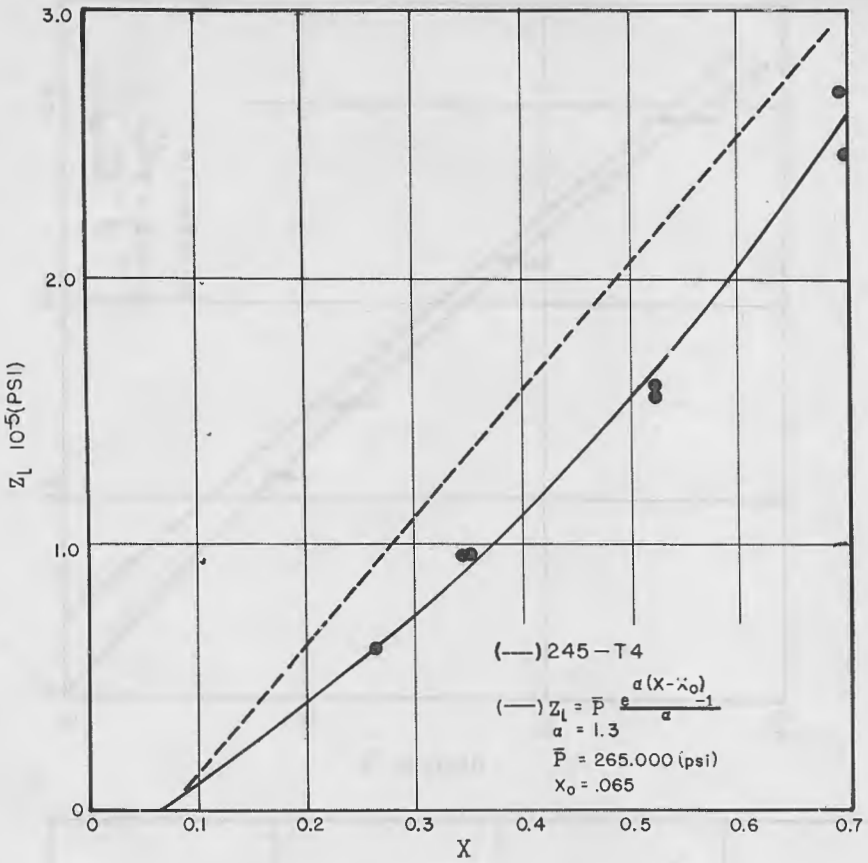

Figure 19 - Alloy Type I, heat No. 2394, Z_L vs. X

The performance curves of the Mg-Li heats fabricated in a range of thicknesses were displayed in Figures 15 through 19. These plots also contain a straight line which refers to fragment penetration resistance of World War II quality 24S-T4 aluminum alloy sheet. This latter material was commerical production and hence provides a good basis for comparison of 22-caliber yawed-dart performance. It should be emphasized that laboratory samples of specially prepared aluminum-based alloys have been tested which show a performance which plots above this 24S-T4 line.

Any comparison of fragment armor performance which is to be of practical value must be made at equal armor weights. It is primarily the weight of armor which limits its use in service. Secondary considerations often result in certain limitations being placed by armor designers on maximum bulkiness, or minimum section rigidity and similar quantities, but these are usually less stringent than the allowable armor weight per unit area to be protected.

When the performance of an armor exhibits curvature in a region of areal density (weight per unit area) of practical interest, as do Mg-Li alloys, nylon cloth laminates and many other newer fragment armor materials, it is quite difficult, if not impossible, to reduce the performance of the material relative to some arbitrary standard material to a single number indicating relative superiority or inferiority. We shall make no attempt to develop a rational basis of comparison. Instead, we shall compare arbitrarily the performance

of Mg-Li alloy types discussed in this report at a value of the performance of 24S-T4 aluminum corresponding to a value of the parameter X = 0.6. This parameter expresses the ratio of the mass of the plate material shadowed by the missile during penetration to the mass of the missile—it may be termed the relative plate mass. The level of performance (αV_L^2) at which we choose to make comparisons is that corresponding to the limit velocity of an aluminum alloy plate (density = 2.8 gm/cm^3) having relative mass of X = 0.6. (This is equivalent to a $V_L \approx 2190$ ft/sec and approximately a 1/4-inch 24S-T4 sheet.) The difference in the weight of Mg-Li possessing this level of performance and the weight of 24S-T4 is found by interpolating between observed data points on a Z_L vs. X plot. This difference expressed as a percent is obtained from the following formula:

$$\text{Wt. Saving (\%)} = 100\ \frac{X_{Al} - X_i}{X_{Al}}$$

where X_{Al} is chosen equal to 0.6 and X_i corresponds to X values for equal Z_L of the material being compared. (Z_L arbitrarily equals 205×10^{-3} psi). The results so obtained for the various Mg-Li alloys are summarized in Table 15 below. Negative saving indicates performance which is inferior to 24S-T4, under the conditions given above. It will be noted that this method for comparison shows that 6 Mg/Li, 6% Al alloy possessed the greatest weight saving over 24S-T4 aluminum alloy under these somewhat arbitrary conditions of comparison. The relative rating of the heats listed in Table 15 will not be altered if the comparison is made at other levels of performance of 24S-T4 but the quantitative comparisons will change appreciably. Further, it should be emphasized that this comparison of performance is based on fragment-like penetration data—the relative rating of the various alloy types against armor piercing projectiles may be altered to favor the harder alloys. At present there is no information available on the armor piercing penetration resistance of Mg-Li alloys but such is expected to be obtained shortly by the Naval Proving Ground on certain thick (1 - 1-1/2 inch) Mg-Li alloy plates.

TABLE 15

Probable Weight Saving Afforded by Mg-Li Alloy Armours over 24S-T4 Aluminum Alloy

Alloy Type	Heat No.	% Wt. Saving (at X = 0.6)
I	2211	Negative
I	2394	Negative
II	2212	8 %
III	No thickness variation available	
IV	2391 (Binary Mg-Li)	5 %
IV	2213	17 %

SUMMARY AND CONCLUSIONS

This report describes the fragment penetration resistance of four Mg-Li alloy types being developed in cooperation with the Battelle Memorial Institute under BuAer Contract NOa(s) 9526. The principal results may be summarized as follows:

(1) The simpler 6 Mg/Li 6% Al alloy is found to possess the greatest weight saving of the Mg-Li alloys over the weight of 24S-T4 aluminum alloy plate having equal ballistic performance.

(2) The better Mg-Li-based alloys exhibit more curvature in plots of limit energy vs. armor thickness than do other metal armors studied to date.

(3) Those alloys exhibiting the highest fragment performance also exhibit deep drawing and bulging in the behind the plate deformation, no spalling, and essentially no plugging. This type of back of plate performance has not been observed previously in homogeneous metal fragment armors.

(4) The fragment performance of the Mg-Li alloys studied does not correlate with slow-speed mechanical properties of the alloys.

(5) The performance of the alloys studied does appear to correlate, qualitatively with the density of the alloys—the higher performance is observed for the alloys of lower density. However, there are effects other than density which affect the performance. These are not discussed in the present report.

(6) Metallographic studies of the alloys have not progressed far enough to attempt to correlate the microstructure of the alloys with ballistic performance. Some preliminary results for one alloy will be presented in a forthcoming report.

RECOMMENDATIONS FOR FUTURE WORK

1. There are certain systematic variations in fragment performance with variations in solution and precipitation heat treatment which can be noted by careful study of the ballistic and nonballistic properties of the alloys described in this report. The source of these variations should be carefully traced and reasons for the performance differences ascertained if possible. It is planned to discuss these effects in a forthcoming report.

2. Certain of the plates show higher mechanical (ballistic and nonballistic) performance in the transverse direction (heat 2044). A systematic survey of anisotropic effects should be undertaken to ascertain degree of variation in performance to be expected from Mg-Li alloy armors.

3. In spite of the extremely low slow-speed indentation hardnesses,* it is not improbable that Mg-Li alloys will possess a considerable penetration resistance (perhaps connected with the high apparent α values) against AP projectiles. Thicker plates of all promising compositions ($\alpha > 0.7$, say) should be subjected to 50-caliber attack at normal and high obliquities. Note added in proof: Thick plates of alloy Type I have been fired recently at NPG and this Laboratory (NRL) with 50-caliber AP projectiles. The plates appear to have a performance, at normal obliquity, quite comparable with 24S-T4.

4. Fundamental studies should be initiated to reveal the role played by Li in modifying the mechanical behavior of magnesium. This could probably best be done by studying the ballistic and nonballistic properties of binary Mg-Li alloys for weight ratios varying from, say, 90 to 5.

ACKNOWLEDGMENTS

The authors wish to acknowledge the many helpful discussions on the metallurgical aspects of this report with Messrs. Eastwood, Frost, and Lorig of the Battelle Memorial

* Brinell hardness of 40 - 100 BHN

Institute, as well as their fine care in the preparation of the experimental material and their assistance in obtaining the nonballistic properties incorporated in this report. Similarly, acknowledgment is made of the many stimulating discussions held throughout the past years with Dr. G. R. Irwin on the general topic of penetration dynamics. It was he who originally suggested the general framework of the method of analysis used in this report. In addition, they wish to express their appreciation to Dr. W. H. Sanders and Miss A. M. Sullivan of the Mechanics Division, NRL, for their patience in reviewing the manuscript and for their many valuable suggestions. We are indebted to the NRL Graphic Arts Branch for many of the illustrations and for assistance in preparing the graphical displays.

* * *

NAVY-DPPO PRNC. WASH., D.C